PAPER • OPEN ACCESS

Characterization of brushed dc motor with brush fault using thermal assessment

To cite this article: A A Wahab and M A H Rasid 2020 *IOP Conf. Ser.: Mater. Sci. Eng.* **788** 012095

Characterization of brushed dc motor with brush fault using thermal assessment

A A Wahab[1] **and M A H Rasid**[1]

[1] Faculty of Mechanical Engineering, Universiti Malaysia Pahang, 26600, Malaysia

*Corresponding author: mahizami@ump.edu.my

Abstract. Direct current motors (DC motor) are used in the small electric devices commonly. Brushed DC motors are cheap and easy to install, thus their popularity. Although the popularity, faults occur which make diagnosis and detection of faults very important. It avoids financial loss and unexpected shutdown operation causes by these faults. This paper is a present characterization of brushed DC motor with brush fault using thermal signature analysis. To organize the character, the temperature profile of DC motor was analysed using the K-type thermocouple with data logger. The thermocouples were mounted on 4 part of the DC motor, casing, permanent magnet, brush and bearing. The temperature data of DC motor with faulty brush and healthy DC motor were measured by thermocouple and recorded using data logger in real time until steady state temperature, under different load. The analysis on the steady state temperature of brush fault can be conclude through recognisable of characteristics temperature difference with a healthy motor.

Keywords. Fault diagnosis; Thermal behaviour; Temperature profile; Brushed dc motor; Brush fault

1. Introduction

DC motor is the most popular motor used in simple onboard application. Several applications with low power (under 250W) in a very large range of field use DC motor. Considered by simple assembly and control, it is largely used even by hobbyist, in electrical learning starter kit on electro-mechanical energy conversion demonstrator and for modular add-on electrical systems [1]–[4]. Typical applications of brushed DC motors are in the low voltage ranging from 12-24 V, as found in cost-effective creations for drone, e-bike, scooter and also automotive drives. These drives are so prevalent that as many as 80 single drives are installed in each of today's luxury cars.

Many researches about Fault Detection and Diagnosis (FDD) of electric motor presented various type of method with different of common fault. The common fault of electric motor can divide by two categories. First is mechanical fault such as bearing fault, eccentricity fault, rotor shaft bending, commutator fault, brush fault (shown in figure 1) and ventilation system problem [5]–[7]. Generally, thermal signal analysis used to detect mechanical fault on electric motor. The other category is electrical fault it including stator winding fault, rotor broken bar, wire insulated damage and external sensor devices [8]–[10]. Indeed, the most recurrent faults which can be found in the stator part such as short circuits between turns or between phases commonly due to an abnormal elevation of

IOP Conf. Series: Materials Science and Engineering **788** (2020) 012095 doi:10.1088/1757-899X/788/1/012095

temperature. This can bring insulation degradation, or even in the worsts case short circuit and irreversible damage [11]–[13]. The same application of thermal assessment for electrical fault as in mechanical fault can be sometime difficult due to inherent nature of Joule losses in conductors. Therefore, plenty other method also exists.

Several technique of FDD methods of electric motors can be found in the newest review [10]–[13]. Different of FDD technique for various fault were proposed [14]–[18]. Normally brush fault are related to brush carbon broken and wiring of brush have damage that will make the brush not functional. Other FDD techniques that can be cited are based on various signals such as: electric current or motor current signal analysis [19]–[21], vibrations signal analysis [22]–[24], acoustic signals analysis [25]–[27], thermal signal analysis [28], [29].

Figure 1. One of brush carbon is broken in (red round).

2. Proposed techniques of characterized temperature

Figure 2 show the experiment setup of Dynamometer test bench. Temperature is a physical parameter that showing the existence of energy in form of heat. Electric motor generated heat from Copper Losses caused of the current flow passing through the conductors. It can be quantified using equation (1).

$$P_{copper} = R.I^2 \tag{1}$$

From the equation 1, shows the losses are proportional to the resistance of the conductor R, which is the winding of the motor in the case of electrical machine and also proportional to the current square. In principle, the speed of a motor is proportional to the voltage, while the torque is proportional to the current as presented in equation (2) and equation (3).

$$V=I.R+E \ ; \ E=k_E.\omega \tag{2}$$

$$T=k_T.I \tag{3}$$

Thus, as the load increase, the current increase and cause in consequence higher losses. In this paper, the speed will be maintained as a constant parameter by keeping the voltage apply to the electric motor at 5V. The current as a changing parameter, and it will be adjusted by changing the load. The brushed DC motor used in this study has the parameters as listed in the table 1 below:

Table 1. Specifications of the Brushed DC motor studied.

Specification	Detail
Model	MY1016
Voltage	240 VDC
Rated speed	2650 RPM
Rated current	13.7 A
Output	250 W

The brushed DC motor was instrumented by thermocouple as a temperature sensor on its bearing, brush, permanent magnet and casing.

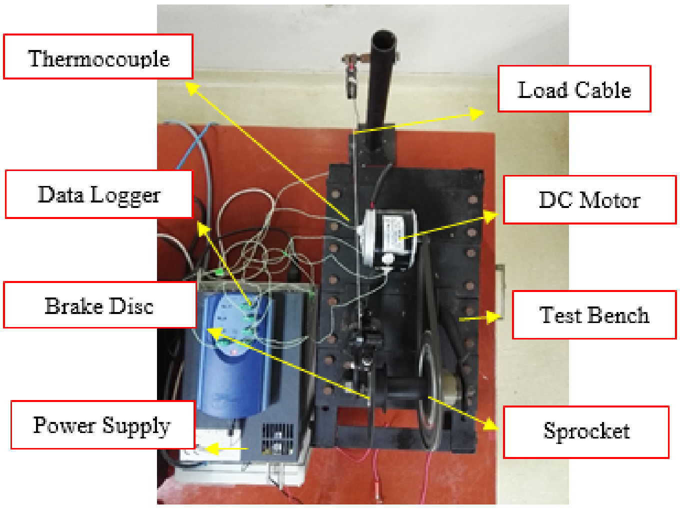

Figure 2. Experiment setup of Dynamometer test bench.

3. Methodology

Figure 3 show the methodology flow chart of the experimental procedure. The first step starts with instrumenting the motor with thermocouple on the component to be monitored. The most important part is the brush. Other parts are also instrumented in order to be compared with. They are casing, permanent magnet, and bearing. After completed, the motor is installed on the test bench as shown in figure 2, and the thermocouples are attached to the data logger that record and display the temperature on a monitor in real time. The load is then applied to by attaching a mass that pull on a brake system that apply a counter torque to the motor shaft. Then, the motor is switched on and accelerated to the reference speed which is set at 5V. Two sets of motor (healthy and faulty brush) were tested under the condition of speed and load parameter as listed in table 2 below. The healthy and faulty bearing motor are compared under the same speed at different loading.

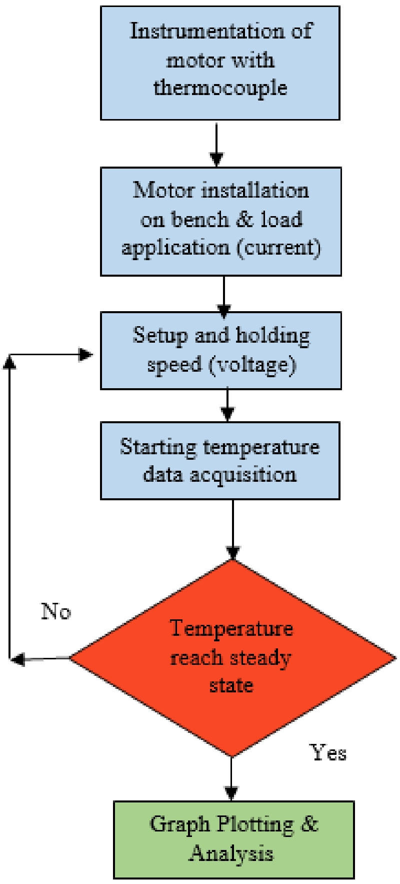

Figure 3. The methodology flow chart of temperature profile experiment procedure.

Table 2. Speed and load parameter of experiment.

Speed ∝ Voltage (Volt)	Loading	Load ∝ Current (Ampere)
5V	No-load	0.5A
5V	With load	1.5A

Once the speed and load set, then the data acquisition of the temperature rise start to be recorded until the steady state reached. After the steady state reached, the data recorded are analyzed and graph plotted using the data. The motor is finally unplugged from the power supply and leave to cool down back to the ambient temperature. All of experiment will repeat several times to make sure the validation and consistently of data.

4. Results and discussion

The temperature data recorded for both healthy and faulty brush motor are then plotted and shown in figure 4 and figure 5.

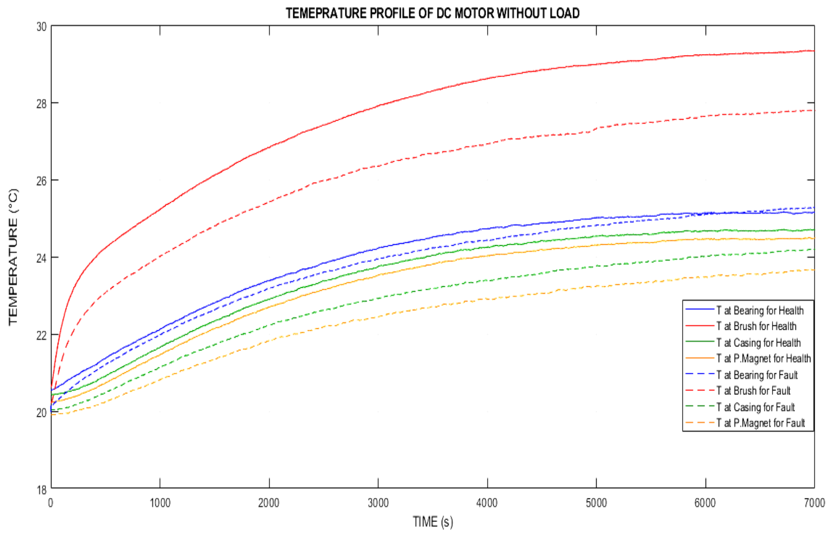

Figure 4. Temperature profile of healthy and faulty brush motor at no-load.

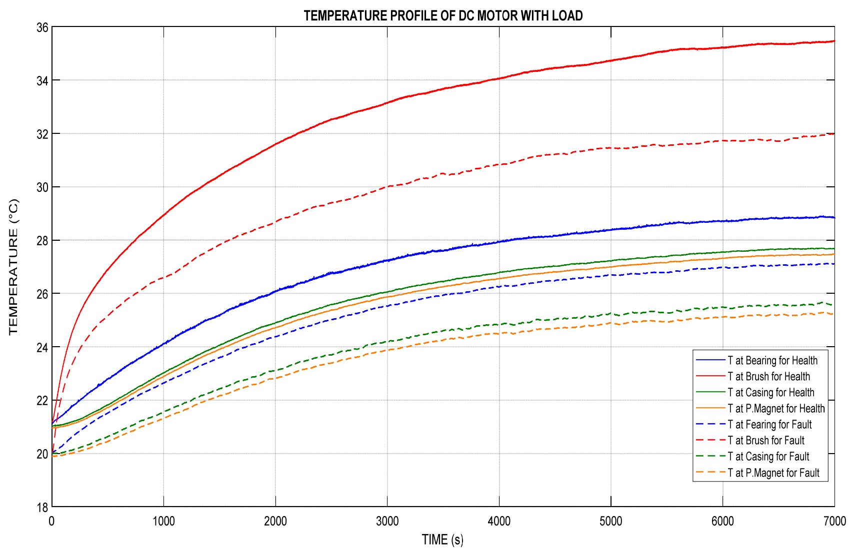

Figure 5. Temperature profile of healthy and faulty brush motor at load.

First things that can observed is all of the components take around 7000 seconds to reach steady state temperature. For cool down time of all component to get back the ambient temperature also same. The steady state temperature, regardless the loading and fault, are in descending order started with the brush, the bearing, the casing and the permanent magnet. The highest temperature is brush component as expected, because brush as an electrical component that conduct current from the power supply to the rotating commutator that deliver the current to the stator of the motor. Therefore, both influence of mechanical friction and copper losses lead to very high temperature. Table 3 presents more detail about steady state temperature analysis for steady state temperature of heathy DC motor at different load and for steady state temperature of DC motor with faulty brush also presented at table 4.

On the right column of both tables, the temperature increase in percentage of the comparison between no-load and loaded case are presented. Accordingly, a bar chart presenting it is drawn in figure 6.

Table 3. Steady state temperature of healthy motor at different load.

DC motor part	Temperature for 0.5A DC motor (°C)	Temperature for 1.5A DC motor (°C)	Temperature Increase (°C) / %
Bearing	25.15	28.88	3.73 / 14.83
Brush	29.33	35.47	6.14 / 20.93
Casing	24.71	27.68	2.91 / 12.02
P.Magnet	24.48	27.47	2.99 / 12.21

Table 4. Steady state temperature of motor with faulty brush at different load.

DC motor part	Temperature for 0.5A DC motor (°C)	Temperature for 1.5A DC motor (°C)	Temperature Increase (°C) / %
Bearing	25.27	27.11	1.84 / 7.28
Brush	27.79	31.98	4.19 / 15.08
Casing	24.20	25.61	1.41/ 5.83
P.Magnet	23.66	25.24	1.58 / 6.68

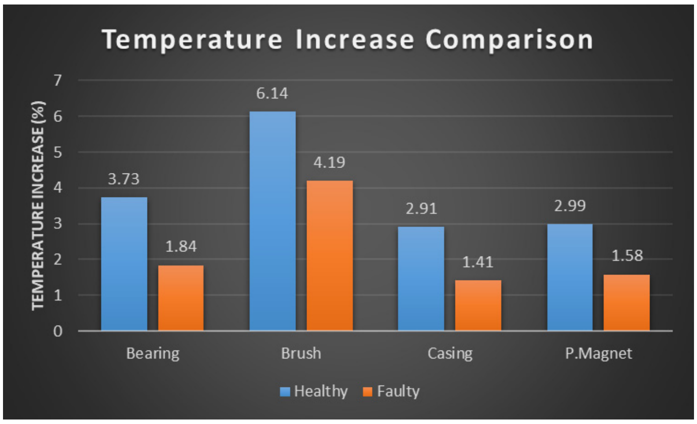

Figure 6. Temperature increase in percentage (%) of the comparison between no-load and loaded case.

In general, from figure 6, from observation that the temperature difference increases from the case no load with the case loaded is obviously higher for the motor with healthy compare to the DC motor with brush fault. That because of one pair of brush carbon on fault DC motor are not function. So performance of fault DC motor lower than health DC motor which causes temperature for health DC motor is higher than fault DC motor. The detail of temperature comparison between healthy and faulty motor at both no-load and loaded (table 5), that the temperature difference of healthy and faulty motor is very small in the case without load throughout the components. None is abnormally higher compared to others. Therefore, at no load, faulty brush cannot be detected.

IOP Conf. Series: Materials Science and Engineering **788** (2020) 012095 doi:10.1088/1757-899X/788/1/012095

In table 5 shows, the different temperature does not have a large gap between motors part. But in the same time, the temperature profile of health DC motor are higher than temperature profile of brush fault DC motor on all of measured component.

Table 5. Temperature different (Δ Temperature) of DC motor between healthy motor and faulty bearing under no load and under load.

Part of DC motor	Δ Temperature (°C) (Healthy-Faulthy)	Different Temperature	Part of DC umotor
Bearing	Without load	With load	1.84 / 7.28
Bearing part	-0.12	1.77	Bearing part
Brush part	1.54	3.49	Brush part
Casing part	0.51	2.07	Casing part

5. Conclusions

The first conclusion that can be made is that faulty brush due to broken one of carbon brush low performance of DC motor and decrease overall motor component temperature. Brush fault hard to distinguish when motor operate at no load condition but, the performance of DC motor can be recognized when motor operate in load condition. The temperature level on the brush and other 3 components of brushed DC motor with brush fault are clearly lower to compare with healthy brushed DC motor. Therefore, a brush fault diagnosis and characterize can be done using thermal analysis on a loaded motor. A larger test on a more extensive and higher range of load would certainly put forward the brush fault.

In a perspective, the proposed diagnostic and characterize technique can be extended to higher power electric motor. In the future, we will analyze more high powers electric motors and other faults with various operational parameters. Lastly, a standard temperature table related to load can be developed to help a faster diagnostic

Acknowledgement

The authors would like to thank Ministry of Higher Education Malaysia for providing Research Acculturation Grant Scheme (RAGS) under project number RDU160397 and also UMP Postgraduate Research Grants Scheme (PGRS) under project number PGRS190328. Special thanks to Universiti Malaysia Pahang for providing laboratory facilities and technical support for this research.

References

[1] M. N. Modreanu, M. I. Andrei, C. Boboc, and M. Morega, 2015 "Unitary design of small DC motors used in modular add-on electrical systems," 2015 *9th Int Symp Adv Top Electr Eng ATEE 2015*, pp. 188–192.

[2] A. Consoli, A. Bottiglieri, R. Letor, R. Ruggeri, A. Testa, and S. De Caro, 2004 "Sensorless position control of DC actuators for automotive applications," Conf Rec 2004 IEEE Ind Appl Conf 2004 39th IAS Annu Meet, vol. 2, pp. 1217–1224 vol.2.

[3] W. S. Ra, H. J. Lee, J. B. Park, and T. S. Yoon, 2008 "Practical pinch detection algorithm for smart automotive power window control systems," *IEEE Trans Ind Electron*, vol. 55, no. 3, pp. 1376–1384.

[4] F. Baronti, F. Lenzi, R. Roncella, and R. Saletti, 2008 "Sensorless control of the suspension preload in motorcycles BT - 2008 *IEEE International Symposium on Industrial Electronics, ISIE 2008*, June 30, 2008 - July 2," pp. 1125–1424416655.

[5] D. Necula, N. Vasile, and M. Stan, 2012 *"Electrical Machinery Defectsand Diagnosis Methods,"* vol. 2, no. 5, pp. 292–296.

[6] M. Iorgulescu and R. Beloiu, 2012 "Study of DC motor diagnosis based on the vibration spectrum and current analysis," 2012 *Int Conf Appl Theor Electr ICATE 2012 –* Proc.
[7] P. Redón, M. . Picazo-Ródenas, R. J. Romero-Troncoso, and J. Antonino-Daviu, 2017 "Reliable methodology for online fault diagnosis in induction motors using passive infrared thermography," 2017 *IEEE 11th Int Symp Diagnostics Electr Mach Power Electron Drives*.
[8] Y. L. Karnavas, I. D. Chasiotis, and A. Vrangas, "Fault Diagnosis of Squirrel-Cage Induction Motor Broken Bars based on a Model Identification Method with Subtractive Clustering."
[9] H. Abdallah and K. Benatman, 2017 "Stator winding inter-turn short-circuit detection in induction motors by parameter identification," *IET Electr Power Appl*, vol. 11, no. 2, pp. 272–288.
[10] S. Nandi, H. A. Toliyat, and X. Li, 2005 "Condition monitoring and fault diagnosis of electrical motors - A review," *IEEE Transactions on Energy Conversion*, vol. 20, no. 4. pp. 719–729.
[11] D. Basak, A. Tiwari, and S. P. Das, 2006 "Fault diagnosis and condition monitoring of electrical machines - A review," in *Proceedings of the IEEE International Conference on Industrial Technology*, pp. 3061–3066.
[12] S. Bindu and V. V. Thomas, 2014 "Diagnoses of internal faults of three phase squirrel cage induction motor - A review," in *Proceedings of the 2014 International Conference on Advances in Energy Conversion Technologies - Intelligent Energy Management: Technologies and Challenges, ICAECT 2014*, pp. 48–54.
[13] D. Lopez-Perez and J. Antonino-Daviu, 2016 "Application of infrared thermography to fault detection in industrial induction motors: Case stories," Proc - 2016 *22nd Int Conf Electr Mach ICEM 2016*, pp. 2172–2177.
[14] P. A. Delgado-Arredondo, D. Morinigo-Sotelo, R. A. Osornio-Rios, J. G. Avina-Cervantes, H. Rostro-Gonzalez, and R. de J. Romero-Troncoso, 2017 "Methodology for fault detection in induction motors via sound and vibration signals," *Mech Syst Signal Process*, vol. 83, pp. 568–589.
[15] P. Kripakaran and B. R. Reddy, 2017 "Diagnosis of bearing fault in induction motor by zero sequence current," in 2017 *International Conference on Innovative Research in Electrical Sciences*, IICIRES 2017, no. 7.
[16] D. López-Pérez and J. Antonino-Daviu, 2016 "Detection of mechanical faults in induction machines with infrared thermography: Field cases," *IECON Proc (Industrial Electron Conf*, pp. 7107–7112.
[17] J. R. Stack, T. G. Habetler, and R. G. Harley, 2004 "Bearing fault detection via autoregressive stator current modeling," *IEEE Trans Ind Appl*, vol. 40, no. 3, pp. 740–746.
[18] R. Razavi-Far, M. Saif, V. Palade, and E. Zio, 2017 "Adaptive incremental ensemble of extreme learning machines for fault diagnosis in induction motors," 2017 *Int Jt Conf Neural Networks*, pp. 1615–1622.
[19] D. Zhen, T. Wang, F. Gu, and A. D. Ball, 2013 "Fault diagnosis of motor drives using stator current signal analysis based on dynamic time warping," *Mech Syst Signal Process*, vol. 34, no. 1–2, pp. 191–202.
[20] Mohammad Rezazadeh Mehrjou, N. Mariun, M. H. Marhaban, and N. Misron, 2010 "Fourier analysis of motor current for diagnosis of broken bars in squirrel-cage induction machines," 2010 *IEEE Student Conf Res Dev*, no. SCOReD, pp. 475–478.
[21] H. Nakamura, T. Oono, and Y. Mizuno, 2008 "Analysis of Current Waveforms of Induction Motors with Short Circuit Faults," 2008 *Annu Rep Conf Electr Insul Dielectr Phenom*, pp. 56–59.
[22] B. Li, G. Goddu, and M. Y. Chow, 1998 "Detection of common motor bearing faults

using frequency-domain vibration signals and a neural network based approach," in *Proceedings of the American Control Conference*, vol. 4, pp. 2032–2036.

[23] G. Betta, C. Liguori, A. Paolillo, and A. Pietrosanto, 2002 "A DSP-based FFT-analyzer for the fault diagnosis of rotating machine based on vibration analysis," *IEEE Trans Instrum Meas*, vol. 51, no. 6, pp. 1316–1321.

[24] M. Iorgulescu, R. Beloiu, and M. O. Popescu, 2010 "Rotor bars diagnosis in single phase induction motors based on the vibration and current spectrum analysis," 2010 12th *Int Conf Optim Electr Electron Equip*, pp. 364–370.

[25] S. Lu, X. Wang, Q. He, F. Liu, and Y. Liu, 2016 "Fault diagnosis of motor bearing with speed fluctuation via angular resampling of transient sound signals," *J Sound Vib*, vol. 385, pp. 16–32.

[26] A. Glowacz, W. Glowacz, Z. Glowacz, and J. Kozik, 2018 "Early fault diagnosis of bearing and stator faults of the single-phase induction motor using acoustic signals," *Measurement*, vol. 113, no. May 2017, pp. 1–9.

[27] P. Sharma and N. Saraswat, 2015 "Diagnosis of Motor Faults Using Sound Signature Analysis," *Ijireeice.Com*, vol. 3, no. 5, pp. 80–83.

[28] A. Glowacz and Z. Glowacz, 2017 "Diagnosis of the three-phase induction motor using thermal imaging," *Infrared Phys Technol*, vol. 81, pp. 7–16.

[29] A. Glowacz and Z. Glowacz, 2016 "Diagnostics of stator faults of the single-phase induction motor using thermal images, MoASoS and selected classifiers," *Meas J Int Meas Confed*, vol. 93, pp. 86–93.